Research Journal of Engineering Sciences ISSN 2278 – 9472
Vol. **12(3),** 6-14, September **(2023)** *Res. J. Engineering Sci.*

Study of the physical and mechanical properties in volume of TiAl by the MEAM method (B1, B2 and L10)

Yahnn J MIGHENSLE MIMBOUI[1,2,4*], Alain S DZABANA HONGUELET[1,2,4] and Timothée NSONGO[1,2,3]
[1]Faculty of Science and Technology, Marien Ngouabi University, Congo Brazzaville
[2]Research Group on Physical and Chemical Properties of Materials, Congo Brazzaville
[3]Geological and Mining Research Center, Congo Brazzaville
[4]Association Alpha Sciences Beta Technologies, Congo Brazzaville
mimbouiyahnn@gmail.com

Available online at: www.isca.in, www.isca.me
Received 26th March 2023, revised 23rd May 2023, accepted 15th June 2023

Abstract

In this work, we present the results of our study on the physical and mechanical properties in volume of the Ti-Al binary alloy system. This work consisted in determining the physical and mechanical properties of different crystallographic structures (L10, B1 and B2) of the Ti-Al alloy using the Modified Embedded Atom Method (MEAM) as well as the MEAM potentials of titanium, aluminum and Ti-Al interaction. We used the LAMMPS calculation code, based on classical molecular dynamics, to determine the most stable structure of TiAl which remains the L10 structure with crystal parameters a=4.02Å and c=4.10Å followed by the B2 structure with parameter a=3.23Å. We also found that the B2 structure has more possibility of transiting to other structures. We have shown that the mechanical behavior of some structures are preferable to others such as L10 and B1 resist compression best while B2 resists stretching, The results (some) obtained, during this study, were calculated by other methods (DFT) compared with the theoretical results and show a considerable agreement.

Keywords: MEAM, LAMMPS, Code, Molecular dynamics, Elastic constants, Modules, Ovito, titanium nitride.

Introduction

For several years, alloys based on the intermetallic compound TiAl have been of growing interest in the scientific community, with a view to structural applications in the aeronautical and automotive sectors. Thanks to their properties, they can also be candidates with high potential and play a key role in military applications (ballistics, armor).

TiAl alloys are intermetallics, with a long-range ordered crystallographic structure. The interatomic bonds are not only metallic, but also covalent, which gives them high strength but also brittleness. The main characteristic of these alloys is to combine a low density (≈ 4 g/cm^3), about half that of superalloys (≈ 8 g/cm^3), with high mechanical strength at high temperatures, and good oxidation resistance. These properties give this material great potential in high-temperature industrial, aerospace and automotive applications[1,2].

Antoine PARIS has worked on the study of Phase Transformations in TiAl base alloys with low silicon alloys[3]. The objective of his work was to increase the knowledge related to the precipitation of silicides in titanium aluminides, in order to be able to propose a metallurgical route implementing in an optimized way this structural transformation to, if necessary, improve the mechanical properties of these alloys. To do so, he contributed to develop the knowledge of the phase equilibria in the Ti-Al-Si ternary system. He then characterized the structural modifications of four compositions of alloys, during their solidification and then during solution and precipitation heat treatments.

Sandrine AMELIO led the studies on the microstructural evolution of a TiAl based alloy. Mechanical stress by dynamic compression and thermal stability[4]. This study led to the study of the microstructural evolution of an intermetallic alloy based on TiAl during mechanical solicitations by dynamic compression as well as its behaviour during isothermal thermal treatments. The TiAl based alloy studied is characterized by good mechanical properties at high temperature and by a low density.

Professor Timothée NSONGO studied the order-disorder transformation of the TiAl binary alloy system by numerical simulation using the EAM inserted atom method[5]. The aim of this thesis was to determine mainly the influence of the lattice constant, the composition on the type of the order-disorder transformation and the order processes in the alloys.
Mohamed BENHAMIDA has worked on the structural, elastic and electronic properties of transition metal nitride alloys[6]. He studied the structural, electronic and mechanical properties of transition metal nitrides using the DFT density functional theory and compared with experimental results.

The aim of our work is to study the Ti-Al alloy system in different structures by computer simulation under the Lammps

code based on molecular dynamics using the Modified Embedded Atom Method to determine the most stable structure. We also studied the mechanical and elastic properties of the alloy.

Methodology

We performed a simulation under the LAMMPS code version 2020 with the executable lmp_mpi, under the Windows operating system, using the MEAM potentials found in the database at https://www.ctcms.nist.gov/potentials/system.

The MEAM potentials of Titanium, Aluminium and Ti-Al interaction used in this work were developed respectively by Y.-M. Kim, B.-J. Lee and M.I. Baskes, M.I. Pascuet and J.R. Fernández and Y.-K. Kim, H.-K. Kim, W.-S. Jung, and B.-J. Lee and are presented in the following two tables[7,8,9]:

These potentials were used to calculate the cohesive energies under different crystallographic structures using the Lammps code and the MPC4 software.

The calculations were simulated for periodic crystallographic structures for 5x5x5 mesh under lammps.

The different crystallographic structures studied in this work are: the CFC structure of the NaCl type (B1), the CC structure of the CsCl type (B2) as well as the L10 structure. The data files allowed us to illustrate the different crystallographic structures through several visualization tools.

Table-1: Complementary parameters of titanium and nitrogen**.**

elt	atwt	alat	β_0	β_1	β_2	β_3	t_0	t_1	t_2	t_3	esub	asub	α	Z	lat	ibar	rozero
Ti	47.88	2.92	2.7	1.0	3.0	1.0	1.0	6.8	-2.0	-12.0	4.87	0.66	4.71	12	hcp	3.0	1 .0
Al	26.98	4.04	3.20	2.6	6.0	2.6	1.0	3.05	0.51	7.75	3.36	1.16	4.68	12	fcc	3.0	1.0

Table-2: MEAM parameters of Ti, Al and TiAl.

	Ti	Al	TiAl
Rc (A°)	4.8	4.5	4.8
Delr	0.1	0.1	0.1
Augt1	0	0	0
Erose_form	2	2	2
Ialloy	2	2	2
Zbl (1,1)	0	0	0
Nn2 (1,1)	1	1	1
Rho0 (1)	1.00	1.00	1.0
Ec (1,1)	4.870	3.36	4.375
Re (1,1)	2.920	2.86	2.80
Alpha (1,1)	4.71945	4.68	5.562
Repuls (1,1)	0.00	0.05	0.0250
Attract (1,1)	0.00	0.05	0.0250
Cmin (1,1,1)	1.00	0.49	0.4900
Cmax (1,1,1)	1.44	2.80	1.4400

Results and Discussion

In the following paragraphs we present the results obtained under the LAMMPS code using the MEAM potentials. These results were also calculated by the MPCV4 application under Windows 10, 64 bits.

The crystalline parameters, elastic constants and moduli translating the structural stability for different TiAl structures are presented below.

Crystalline parameters: The crystal parameters as well as the volumes have been calculated for the structures *L10, B1, B2, Do19 and Do22* and are presented in the Table-3.

The most voluminous structure is structure B1 followed by structure Do22 and finally structure B2 in last position.

Cohesive energy and transition: Cohesive energy: We calculated the cohesion energies in different crystallographic structures for TiAl; we realized that the Do19 structure is the most stable with a cohesion energy of -4.766eV followed by the Do22 structure with a cohesion energy of -4.64eV and in last position the L10 structure with an energy of -4.382eV.

Although the number of atoms per cell increases in some structures, the cohesion energy becomes very large, reflecting the instability of the structure beyond eight (8) atoms per cell.

The structures B1 and B3 are very close, although having the same number of atoms they present very close cohesion energies as well as the mesh parameters.

The MEAM potential of TiAl has allowed us, thanks to the MPCV4 application, to represent the cohesion energies for different structures as shown in the Figure-3.

Transition: We represent in this part the energies per eV/atom related to the phase transitions, these energies translate the energy barriers to be provided by atom to change phases.

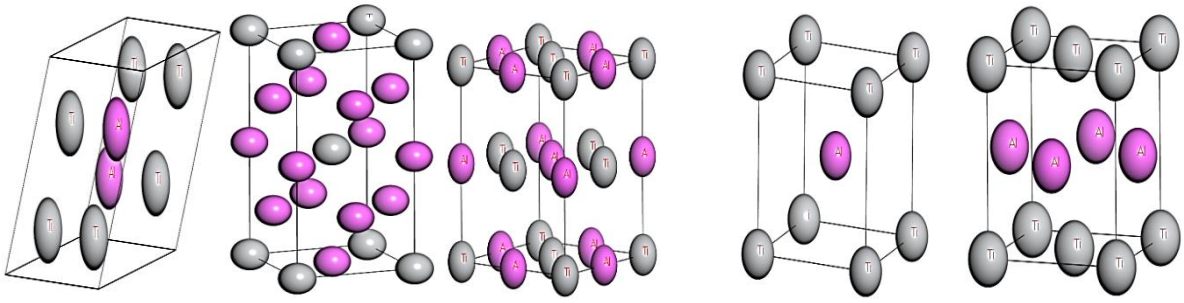

(a) **(b)** **(c)** **(d)** **(e)**

Figure-2: Different crystallographic structures of Ti-Al: a) Ti3Al b) TiAl3 c) TiAl-B1 d) TiAl-B2 e) TiAl-L10.

Table-3: Crystal parameters by structure and crystallographic volume

Structures	a (Å)	b (Å)	c (Å)	Volumes(Å^3)	Theory (Å)[10,11,12,13]		Exp. (Å)[14,15,16,17]
TiAl (L_{10})	4.02	4.02	4.10	66.26	a=b=4.04	c=4.08	a=4.01, c=4.04
TiAl(B1)	5.44	5.44	5.44	160.98	a=b=c=5.5157		-
TiAl(B2)	3.23	3.23	3.23	33.79	a=b=c=3.179		-
$Ti_3Al(Do_{19})$	5.75	5.75	4.65	133.33	a=5.72	c= 4.60	a=5.77, c=4.645
$TiAl_3(Do_{22})$	3.94	3.94	8.81	136.76	a=3.905	c=8.04	a=3.84, c=8.579

Table-3: Cohesive energy per structure of Ti-Al.

Structures	Parameters a(Å)	Total energy(ev)	Ecoh(ev)	Nbre of atoms
TiAl (L_{10})	4.02	-17.53	-4.382	4
TiAl(B1)	5.44	-31.32	-3.915	8
TiAl(B2)	3.23	-8.749	-4.375	2
$Ti_3Al(Do_{19})$	5.75	-38.128	-4.766	8
$TiAl_3(Do_{22})$	3.94	-37.15	-4.64	8

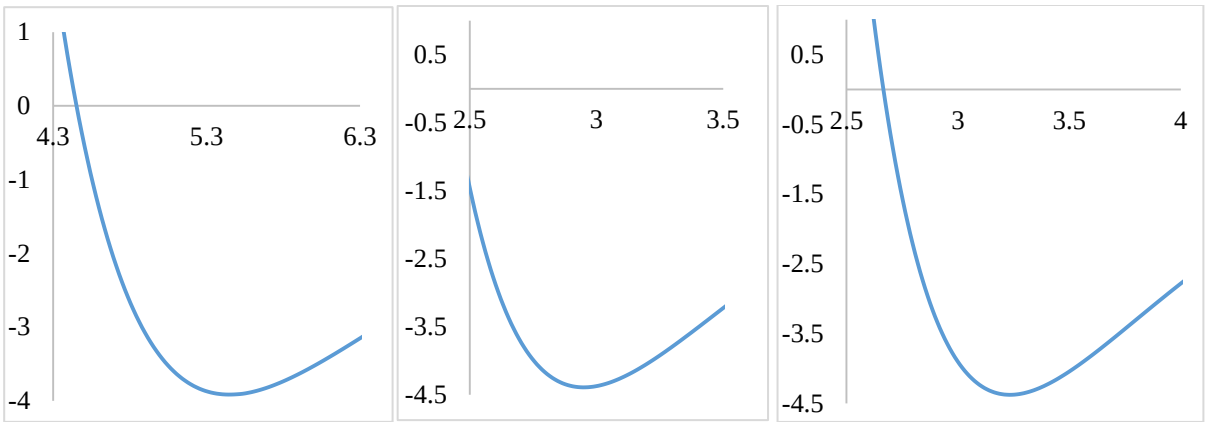

Figure-3: Representative curves of the cohesion energy/crystalline parameter.

Table-4: Transition energy (eV/atom) between Ti-Al structures.

Transition	TiAl (L_{10})	TiAl(B1)	TiAl(B2)	$Ti_3Al(Do_{19})$	$TiAl_3$ (Do_{22})
TiAl (L_{10})		0.605	-1.0925	0.49925	0.515
TiAl(B1)	-0.605		-1.6975	-0.10575	-0.09
TiAl(B2)	1.0925	1.6975		1.59175	1.6075
$Ti_3Al(Do_{19})$	-0.49925	0.10575	-1.59175		0.01575
$TiAl_3$ (Do_{22})	-0.515	0.09	-1.6075	-0.01575	

This study reveals that the B2 structure can undergo phase transitions to all the other structures studied here, followed by the L10 structure and finally the Do19 structure. i. TiAl (L_{10}): can transition to three other structures whose order of transition is by the following relation L10-Do19-Do22-B1; ii. TiAl(B1): is really the most stable structure, it is difficult that it is transformed into another neighboring structure; iii. TiAl(B2): B2 remains the most interesting structure due to the fact that it is the only one that can transit to all the other structures B2-L10-Do19-Do22-B1; iv. Ti_3 Al (Do_{19}): Do19 turns first into Do22 and finally into B1; v. $TiAl_3$ (Do_{22}): on the other hand, Do22 transits only to B1.

It remains reasonable to follow the evolution of the structure of Ti-Al, the opposite effect will be energetically costly.

Mechanical properties: We have calculated for the temperature of 298°K, the elastic constants of TiAl in three different structures B1, B2 and B3 as well as the corresponding elastic moduli.

Elastic constants: The elastic constants c_{ij} are essential parameters for the prediction of elastic properties and mechanical stability of materials.

The elastic and mechanical properties of solids reflect their reactions to the intervention of certain external factors. In the simplest case such factors are mechanical actions: compression, traction, bending, shock, torsion. In addition to mechanical actions, they can be thermal, magnetic, etc.. These properties are determined, in the first place, by the forces of bonds which intervene between the atoms or the molecules constituting a solid.

When subjected to a stress, a crystal deforms linearly with respect to this stress as long as the deformation generated is small. When the stress is removed, the material returns to its standard state in a reversible manner. This behavior observed for all materials is called "elastic".

In order to understand the mechanical stability, we studied the elastic constants at room pressure of TiAl for three different structures such as NaCl (B1), CsCl (B2) and ZnS (B3). The cubic system is characterized by three independent elastic moduli: *C11*, *C12* and *C44*.

For elements that have a cubic structure, the criterion for predicting structural stability is as follows:

$$\boldsymbol{C_{11} - C_{12} > 0,\ C_{11} > 0,\ C_{44} > 0,\ C_{11} + 2C_{12} > 0}$$

And for the elements that have a tetragonal structure, we have this:

$$\boldsymbol{C_{11} > |C_{12}|,\ C_{44} > 0,\ C_{66} > 0,\ C_{33}(C_{11} + C_{12}) > 2C_{13}^2}$$

However, the matrix linking the deformations and the elastic constants is represented by the following relation:

$$\begin{pmatrix}\sigma_1\\ \sigma_2\\ \sigma_3\\ \sigma_4\end{pmatrix} = \begin{pmatrix}C_{11} & C_{12} & C_{13} & C_{14}\\ C_{21} & C_{22} & C_{23} & C_{24}\\ C_{31} & C_{32} & C_{33} & C_{34}\\ C_{41} & C_{42} & C_{43} & C_{44}\end{pmatrix}\begin{pmatrix}\varepsilon_1\\ \varepsilon_2\\ \varepsilon_3\\ \varepsilon_4\end{pmatrix}$$

The constant C_{11} is the measure of the resistance to deformation produced by a stress applied to the (100), (010) and (001) planes along the <100> directions (length elasticity).

C_{44} represents the measure of resistance to deformation in the case of a shear stress applied on the (100), (010) and (001) planes along the diagonals (shape elasticity).

C_{12} has no simple physical interpretation, but these linear combinations with C_{11} give us the compressive modulus B and shear modulus G.

The elastic constants for TiAl structures B1, B2 and B3 have been calculated and are presented in the Table-5.

The exploitation of these data allowed us to compare the elastic constants between them and between the theoretical and experimental data that we represent through, with series 1 for B1 and series 2 for B2 and series 3 for B3; the following Figures-4 and 5.

Table-5: Elastic constants comparison with theory and experiment.

	Elastic constants of Ti-Al in (GPa) : γ-TiAl, Ti_3Al et $TiAl_3$										
	Our work					Theory[18,19,20,21]			Exp.(298°K)[22,23,24]		
	γ-TiAl			Ti_3Al	$TiAl_3$	γ-TiAl, Ti_3Al et $TiAl_3$			γ-TiAl, Ti_3Al et $TiAl_3$		
	L10	B1	B2	DO19	DO22	L10	DO19	DO22	L10	DO19	DO22
C11	161.055	66.13	61.41	189	193	183	185	190	177	175	218
C12	75.563	91.79	170.41	87	86	74.1	83	87	70	88	58
C13	82.268	-	-	64	45	74.4	63	46	72	62	45
C33	162.257	-	-	232	218	178	231	213	171	219	218
C44	109.368	-76.57	75.91	51	94	105	57	96	99	63	92
C66	63.151	-	-	59	129	78.4	51	127	77	-	116

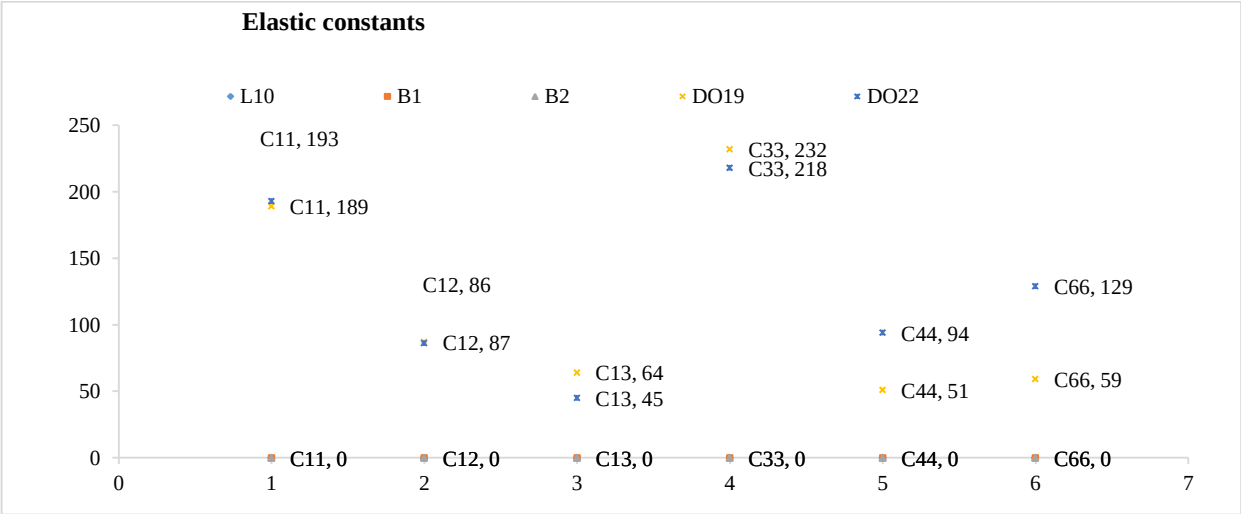

Figure-4: Elastic constants of the B1 B2 and L10 structures of TiAl

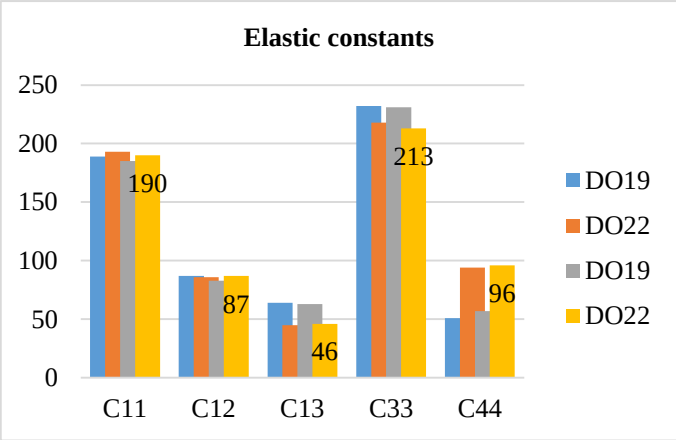

Figure-5: Order of magnitude comparison with experimental data.

The order of magnitude is well defined by C11> C12 and is preserved in the theory as well as for experimental data. Comparing the data, we find that the elastic constants are in the same order of magnitude as the experimental data.

Elastic modules: In this paragraph we present the corresponding elastic moduli in different Reuss Hill and Voigt systems.
These moduli translate the rigidity and flexibility of the material, against external excitations, they translate the directions of the resulting deformation or the resulting stress. We also speak of elastic coefficients which are none other than the moduli of the engineer for the properties of nanomaterials, we give here the mathematical relationships between Young's modulus, compression, Poisson's ratio and shear with the elastic constants. i. The modulus of compression B is defined as the ratio of the hydrostatic pressure to the fractional change in volume produced by that pressure (the volume elasticity). ii. The second modulus *G* is the resistance to deformation produced by a shear stress applied to the plane (110) along the direction [110]. iii. The elastic moduli (Bulk modulus B, Shear modulus G and Young's modulus E) are estimated by the Voigt-Reuss-Hill method. Generally, the larger the B, the greater the resistance of the material to change in volume. iv. The elastic anisotropy A^U plays a vital role in the physical/mechanical process such as fracture behavior and phase transformations[25]. It is given by the following formula[26]:

$$A^U = 5\frac{G_v}{G_R} + \frac{B_v}{B_R} - 6$$

We present in the two tables below all the elastic moduli in different systems of approaches for cubic and hexagonal crystallographic structures.

We considered it appropriate to present the results in two steps according to the relevance of the obtained results, we first present the results related to the L10 structure compared to the theory, then we compared the results with some structures such as B1 and B2 considered interesting. The results obtained from the expressions of the previous modules are presented in the Table-7.

Table-5: Mathematical expressions of elastic moduli for a cubic structure.

$E = \frac{9BG}{3B+G}$	$\nu = \frac{3B - E}{6B}$	$B = \frac{C_{11} + 2C_{12}}{3}$
$G_v = \frac{C_{11} - C_{12} + 3C_{44}}{5}$	$G_R = \frac{5(C_{11} - C_{12})C_{44}}{4C_{44} + 3(\text{﹤}_{11} - C_{12})}$	$G = \frac{G_R + G_V}{2}$
$B_{Hill} = \frac{1}{2}(B_{Reuss} + B_{Voigt})$	$B_R = B_R = \frac{1}{3}(C_{11} + 2C_{12})$	$G_{Hill} = \frac{1}{2}(G_{Reuss} + G_{Voigt})$

Table-6: Mathematical expressions of elastic moduli for a hexagonal structure.

$E = \frac{9BG}{3B + G}$	$\nu = \frac{(3B - 2G)}{(6B + 2G)}$	$B = \frac{C_{11} + 2C_{12}}{3}$
$G = \frac{3c_{44} + c_{11} - c_{12}}{5}$	$C_{66} = \frac{C_{11} - C_{12}}{2}$	$M = C_{11} + C_{12} + 2C_{33} - 4C_{13}$
$B_{Hill} = \frac{1}{2}(B_{Reuss} + B_{Voigt})$	$B_R = \frac{(C_{11} + C_{12})C_{33} - 2C_{13}^2}{C_{11} + C_{12} - 4C_{13} + 2C_{33}}$	$B_V = \frac{2C_{11} + 2C_{12} + 4C_{13} + C_{33}}{9}$
$G_{Hill} = \frac{1}{2}(G_{Reuss} + G_{Voigt})$	$G_R = \frac{5(C_{11} - C_{12})C_{44}}{4C_{44} + 3(C_{11} - C_{12})}$	$G_v = \frac{C_{11} + C_{12} - 4C_{13} + 2C_{33} + 12C_{44} + 12C_{66}}{30}$

The results obtained for the L10 structure in the Voigt system have been compared with the theory and remain in good agreement. These moduli reveal that the L10 structure is very resistant to external stresses, in uniform compression translated by the modulus of compressibility B; its shear modulus E is close to that of steel (81 Gpa), however its anisotropy is considerable compared to that of TiN in B1 structure (0.1625), i.e. that TiAl in L10 structure resists better to breakage than the B1 structure of TiN.

The comparison of the mechanical quantities is given in Table-8.

We note, although having used several programs and codes (DFT, Ab initio) of calculations, the appearance of negative magnitudes for the Young's modulus and shear for B1 in the Voigt system; this translates the behavior in front of the stretching or the compression; we retained that the B1 structure resists to the stretching.

For modules B, G and E; the order of magnitude is maintained for structures L10 followed by B2 and finally B1;

For the λ-module; the order is instead reversed first B2 then B1 and finally L10;

For module v: structure B1 wins against L10 and B2.

These results show us, first of all, that structures L10, B1 and B2 present the same behavior in front of the mechanical constraints, except that structure B1 resists to the stretching rather than the two others which resist to the compression;
Structures L10 and B2 are isotropic because their fish coefficients gravitate around 0.33, while structure B1, which has a considerable fish coefficient, is resistant to shear.

Table-7: Elastic moduli of the L10 structure compared to the theory.

TiAl in L10: Elastic modules (Gpa)						
Size	Symbols	Voigt	Reuss	Hill	Theory[27]	Exp, 298°K[28]
Bulk modulus	B	107.174	107.114	107.144	109.97	110
Shear modulus	G	72.662	59.962	66.312	75.68	
Young modulus	E	177.804	151.599	164.914	184.67	183
Lambda Blade	λ	58.732	67.139	62.936	-	-
Fish Ratio	V	0.223	0.264	0.243	0.220	-
Elastic anisotropy	A^U	1.059			-	-

Table-8: Elastic moduli of structures L_{10}, B1 and B2.

Elastic moduli in structure L10[16], B1, and B2 of γ-TiAl in (Gpa)										
Size	Symbols	Voigt			Reuss			Hill		
		L10	B1	B2	L10	B1	B2	L10	B1	B2
Bulk modulus	*B*	107.174	47.282	119.532	107.114	47.282	119.515	107.144	47.282	119.523
Shear modulus	*G*	72.662	-85.988	19.131	59.962	-55.235	575.555	66.312	-70.611	297.343
Young modulus	*E*	177.804	-655.065	54.486	151.599	-271.380	662.764	164.914	-421.813	487.649
Lambda Blade	λ	58.732	104.608	106.778	67.139	84.106	-264.188	62.936	94.357	-78.704
Fish ratio	*V*	0.223	2.809	0.424	0.264	1.456	-0.424	0.243	1.986	-0.179

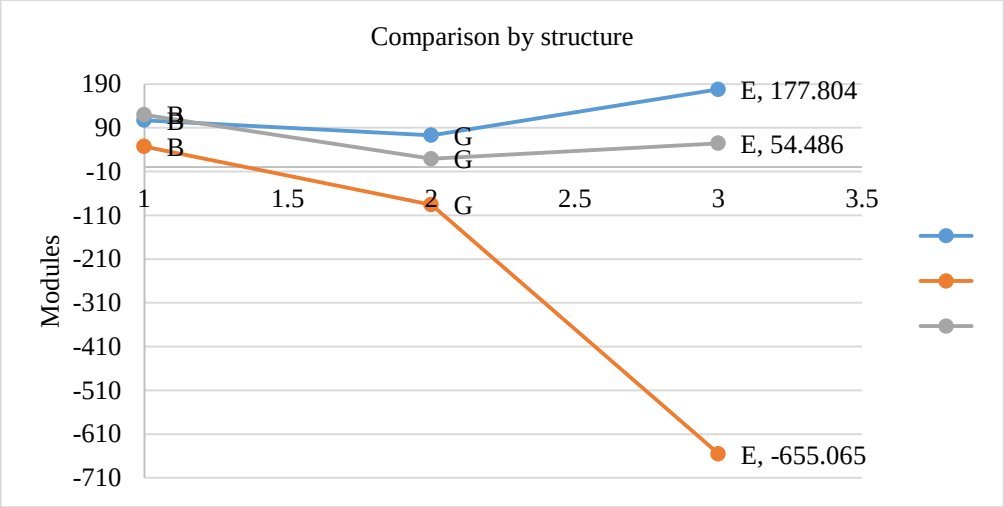

Figure-6: Comparison of modules per structure L10, B1 and B2.

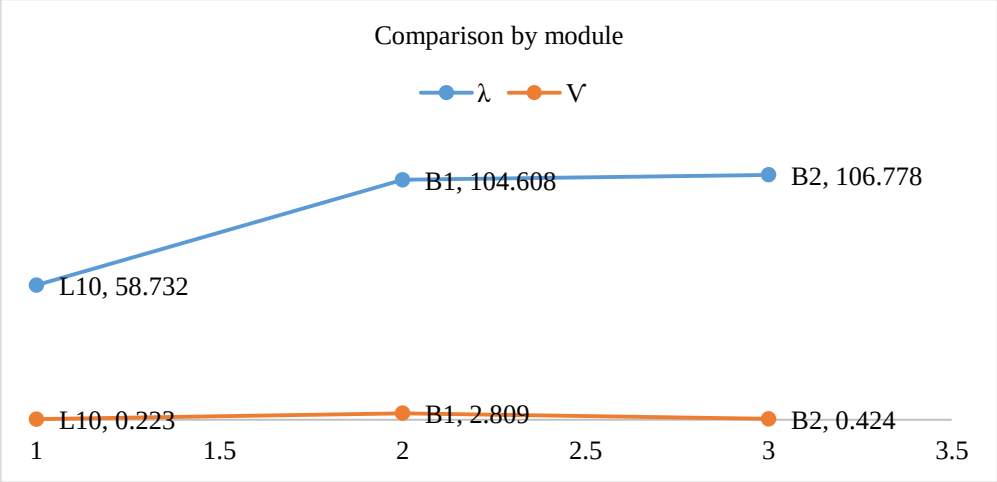

Figure-7: Comparison by modules of structures L10, B1 and B2.

Conclusion

In this work, we have used MEAM potentials to study the mechanical behaviors in front of external stresses of TiAl structures namely L10, B1, B2, Do19 and Do22.

We have thus shown that the number of atoms per cell does not guarantee structural stability, nor the direction of transition between structures. It will be much more interesting to deepen our knowledge of the B2 structure, which presents more possibilities in terms of transition, than the B1 structure for its stability.

The intermediate structures L10, Do19 and Do22 are mechanically stable, satisfying the conditions $C_{11} - C_{12} > 0$, $C_{11} > 0$, $C_{44} > 0$, $C_{11} + 2C_{12} > 0$.

Finally, the highest elastic constants do not guarantee the mechanical properties, only the moduli are essential.

Acknowledgements

We would like to thank the Research Group on Physical, Chemical and Mechanical Properties of Materials (GRPPMM) for allowing us to finalize this work and we would like to thank the Alpha Sciences Beta Technologies association for its support from the very beginning of the writing of this paper.

References

1. Kothari, K., Radhakrishnan, R., & Wereley, N. M. (2012). Advances in gamma titanium aluminides and their manufacturing techniques. *Progress in Aerospace Sciences*, 55, 1-16.
2. Froes, F. H., Kim, Y. W., & Hehmann, F. J. (1987). Rapid Solidification of Al, Mg and Ti. *The Journal of The Minerals, Metals & Materials Society*, 39, 14-21.

3. Antoine PARIS (2015). Study of the Phase Transformations in TiAl base alloys with low silicon alloys. Materials. Université De Lorraine. French. tel-01394655

4. Amélio, S. (2005). Microstructural evolution of a TiAl alloy under dynamic compression and isothermal heat treatment. Doctoral dissertation, Institut National Polytechnique de Lorraine.

5. Nsongo, T., Ni, X., Chen, G., & Chan, K. M. (2001). Order-disorder Transformation for TiAl with L1~ 0 Structure at Stoichiometrical Composition. Rare Metals-Beijing-English Edition, 20(3), 147-151.

6. Mohamed Benhamida (2014). Structural, elastic and electronic properties of transition metal nitride alloys. Ph. D. Thesis. University of Setif 1-Stif.

7. Kim, Y. M., Lee, B. J., & Baskes, M. I. (2006). Modified embedded-atom method interatomic potentials for Ti and Zr. *Physical Review B*, 74(1), 014101.

8. Pascuet, M. I., & Fernández, J. R. (2015). Atomic interaction of the MEAM type for the study of intermetallics in the Al–U alloy. *Journal of Nuclear Materials*, 467, 229-239.

9. Sarkar, S., Datta, S., Das, S., & Basu, D. (2009). Oxidation protection of gamma-titanium aluminide using glass–ceramic coatings. *Surface and Coatings Technology*, 203(13), 1797-1805.

10. Valencia, J. J., McCullough, C., Levi, C. G., & Mehrabian, R. (1987). Microstructure evolution during conventional and rapid solidification of a Ti-50at% Al alloy. *Scripta metallurgica*, 21(10), 1341-1346.

11. Denquin, A. (1994). Etude des transformations de phase et approche du comportment mécanique des alliages biphasés à base de TiAl: une contribution au développement de nouveaux alliages intermétalliques. Doctoral dissertation, Lille 1.

12. Hennig, R. G., Lenosky, T. J., Trinkle, D. R., Rudin, S. P., & Wilkins, J. W. (2008). Classical potential describes martensitic phase transformations between the α, β, and ω titanium phases. *Physical Review B*, 78(5), 054121.

13. Kainuma, R., Ohnuma, I., Ishikawa, K., & Ishida, K. (2000). Stability of B2 ordered phase in the Ti-rich portion of Ti–Al–Cr and Ti–Al–Fe ternary systems. *Intermetallics*, 8(8), 869-875.

14. Banumathy, S., Ghosal, P., & Singh, A. K. (2005). On the structure of the Ti3Al phase in Ti–Al and Ti–Al–Nb alloys. *Journal of alloys and compounds*, 394(1-2), 181-185.

15. Tanaka, K. (1996). Single-crystal elastic constants of gamma-TiAl. *Philosophical magazine letters*, 73(2), 71-78.

16. Pearson, W. B. (2013). A handbook of lattice spacings and structures of metals and alloys: International series of monographs on metal physics and physical metallurgy. Vol. 4 (Vol. 4). Elsevier.

17. Nakamura, M., & Kimura, K. (1991). Elastic constants of TiAl 3 and ZrAl 3 single crystals. *Journal of materials science*, 26, 2208-2214.

18. Tanaka, K. (1996). Single-crystal elastic constants of gamma-TiAl. *Philosophical magazine letters*, 73(2), 71-78.

19. Connetable, D. (2019). Theoretical study of the insertion and diffusivity of hydrogen in the Ti_3Al-D019 system: Comparison with Ti-hcp and TiAl-L10 systems. *International Journal of Hydrogen Energy*, 44(60), 32307-32322.

20. He, Y., Schwarz, R. B., Migliori, A., & Whang, S. H. (1995). Elastic constants of single crystal γ–TiAl. *Journal of materials research*, 10(5), 1187-1195.

21. Liu, Y. L., Liu, L. M., Wang, S. Q., & Ye, H. Q. (2007). First-principles study of shear deformation in TiAl and Ti3Al. *Intermetallics*, 15(3), 428-435.

22. Tanaka, K. (1996). Single-crystal elastic constants of gamma-TiAl. *Philosophical magazine letters*, 73(2), 71-78.

23. Hu, H., Wu, X., Wang, R., Jia, Z., Li, W., & Liu, Q. (2016). Structural stability, mechanical properties and stacking fault energies of $TiAl_3$ alloyed with Zn, Cu, Ag: First-principles study. *Journal of Alloys and Compounds*, 666, 185-196.

24. Nakamura, M., & Kimura, K. (1991). Elastic constants of TiAl 3 and ZrAl 3 single crystals. *Journal of materials science*, 26, 2208-2214.

25. Ledbetter, H., & Migliori, A. (2006). A general elastic-anisotropy measure. *Journal of applied physics*, 100(6).

26. Ranganathan, S. I., & Ostoja-Starzewski, M. (2008). Universal elastic anisotropy index. *Physical review letters*, 101(5), 055504.

27. He, Y., Schwarz, R. B., Darling, T., Hundley, M., Whang, S. H., & Wang, Z. M. (1997). Elastic constants and thermal expansion of single crystal γ-TiAl from 300 to 750 K. *Materials Science and Engineering: A*, 239, 157-163.

28. Tanaka, K. (1996). Single-crystal elastic constants of gamma-TiAl. *Philosophical magazine letters*, 73(2), 71-78.